Cerebral Cortex, December 2018;28: 4365–4378

doi: 10.1093/cercor/bhx290
Advance Access Publication Date: 17 November 2017
Original Article

ORIGINAL ARTICLE

Echoes of Affective Stimulation in Brain connectivity Networks

Viola Borchardt[1,2], Yan Fan[1,3], Marie Dietz[3], Ana Lucia Herrera Melendez[3], Malek Bajbouj[3], Matti Gärtner[3], Meng Li[1], Martin Walter[1,2,5] and Simone Grimm[3,4,6]

[1]Clinical Affective Neuroimaging Laboratory, Magdeburg, Germany, [2]Department of Behavioral Neurology, Leibniz Institute for Neurobiology, Magdeburg, Germany, [3]Charité–Universitätsmedizin Berlin, Corporate Member of Freie Universität Berlin, Humboldt-Universität zu Berlin, and Berlin Institute of Health, Department of Psychiatry, Campus Benjamin Franklin, Berlin, Germany, [4]Department of Psychiatry, Psychotherapy and Psychosomatics, Therapy and Process Research, University Hospital of Psychiatry, Zurich, Switzerland, [5]Clinic for Psychiatry and Psychotherapy, Eberhard-Karls University, Tuebingen, Germany and [6]Medical School Berlin, Berlin, Germany

Address correspondence to Simone Grimm, Department of Psychiatry, Campus Benjamin Franklin, Charité Berlin, Hindenburgdamm 30, 12203 Berlin, Germany. Email: simone.grimm@charite.de

Viola Borchardt, Martin Walter, Simone Grimm, and Yan Fan contributed equally to this work

Abstract

Affective experience has effects on subjective feelings, physiological indices, entails immediate activity changes in the brain, and even influences brain networks in a protracted manner. However, it is still unclear, how the functional connectivity (FC) interplay between major intrinsic connectivity networks upon affective stimulation depends on affective valence, and whether this is specific for affective experience, i.e., can be distinguished from cognitive task execution. Our study included fMRI scans during and after affective stimulation with sad and neutral movies and a working memory task complemented with measures of cardiovascular activity and mood. Via parcellation of the brain into default mode network (DMN), central executive network (CEN), and dorsal attention network, and application of network-based statistics, we identified subnetworks associated with changing psychological contexts. Specific effects for affective stimulation with negative valence were both reduced heart rate variability and mood, and upregulated FC of inter-CEN-DMN connections while intra-DMN connections were downregulated. Furthermore, results demonstrated a valence-specific dynamic carry-over effect in nodes of the CEN, which temporarily increased their FC strength after affective stimulation with negative valence and exhibited distinct temporal profiles. The reported effects were clearly distinguishable from those of a cognitive task and further elucidate the trajectory of affective experience.

Key words: affective stimulation, brain network analysis, dynamics, functional connectivity, resting-state fMRI

Introduction

Affective experience does not start or end instantaneously; carry-over effects of affective stimulation can be found with regard to subjective feelings (Harrison et al. 2008), physiological indices in parasympathetic nervous system (PNS) (Sakuragi et al. 2002), as well as functional coupling in the brain (Eryilmaz

et al. 2011). To understand the affective experience as a whole, these distinct dimensions need to be integrated. In order to achieve this, however, we first need to understand, how affective stimulation influences coupling both within and between different brain networks in a protracted manner.

Intrinsic connectivity networks (ICNs) represent temporally clustered brain regions, which are functionally connected and synchronize their activation depending on environmental demands. One prominent ICN is the default-mode network (DMN), which comprises anterior and posterior medial cortical regions such as pregenual anterior cingulate cortex (PACC) and posterior cingulate cortex (PCC) and is characterized by high resting-state connectivity and activity when individuals direct attention internally, for example, during mind wandering and random thoughts (Gusnard et al. 2001). Activation as well as connectivity of these regions are affected both during affective stimulation and in subsequent resting-state (Harrison et al. 2008; Eryilmaz et al. 2011; Pehrs et al. 2014; Borchardt et al. 2015; Zhang et al. 2015; Schlochtermeier et al. 2017). Recently, Schlochtermeier et al. (2017) have shown, that viewing sad movie scenes engaged activity changes in anterior and posterior cingulate cortex. Further, it has been shown that passive viewing of affective movies engaged activity and connectivity changes not only in the DMN, but also in the central executive network (CEN), as well as in visual and auditory sensory networks (Hyett et al. 2015). Affective stimulation also impacts connectivity of intrinsic neural networks in subsequent resting-state. Such carry-over effects during resting-state after affective movies have been reported with regard to increased ACC-insula connectivity and decreased connectivity within the DMN (Harrison et al. 2008; Eryilmaz et al. 2011). However, previous studies investigated merely coupling between selected regions in ICNs, and changes of connectivity within as well as between different ICNs are yet to be investigated via more systematic network approaches. Borchardt et al. (2015) have applied network-based statistics (NBS) and graph metrics to probe connectivity changes in resting-state after auditory stimuli with affective content and revealed much more intricate network changes between regions in the CEN and DMN. Based on this prior work, it seems promising to use NBS to study connectivity changes within as well as between ICNs that are modulated both during and after affective stimulation.

Barnes et al. (2009) on the question of how after-effects of cognitive activity shape ICN patterns, Barnes et al. have established an interaction between cognitive task performance and subsequent brain oscillations by showing that the recovery rate of endogenous dynamics to baseline (or pretask) values depends on cognitive load. It has been suggested that dynamically varying FC between DMN regions and task-positive regions represents a unique switching behavior that occurs during rest periods after cognitive tasks, suggesting an internetwork interaction pattern that is carried over into resting-state periods (Grigg and Grady 2010). However, it is still unclear whether this might be specific for cognitive stimulation or would also be true for affective stimulation. So far, no studies have investigated effects of both affective and cognitive stimulation on connectivity of intrinsic neural networks in the same subjects.

Regarding physiological and psychological aspects of affective experience, previous research has established a relationship between heart rate variability (HRV) and emotion and demonstrated, that a relative reduction in vagally mediated HRV was consistent with ineffective emotion regulation and poor attentional control (Friedman and Thayer 1998; Thayer and Lane 2000). A sustained effect of sad mood on parasympathetic activity has been suggested because although the high-frequency component of heart rate variability (HF-HRV) gradually decreased during watching comedy and tragedy videos, it did not return to the basal level after watching tragedy videos (Sakuragi et al. 2002). Moreover, it was found that during affective tasks, blood pressure elevated, which indicates hemodynamic responses (Neumann and Waldstein 2001).

HRV, regulation of flexible affective responses, as well as functional connectivity (FC) within the DMN are compromised in depression (Anand et al. 2005; Disner et al. 2011; Hamilton and Alloy 2016). Here, increasing levels of DMN dominance over other ICNs have been associated with higher levels of maladaptive rumination (Hamilton et al. 2011). Rumination is the repetitive focus of attention on negative feelings and thoughts in response to negative mood (Nolen-Hoeksema and Morrow 1991). A predominant tendency to ruminate appears to contribute to pessimism about the future and a negative reflection of the self, which might be a key to affective disorders like depression (Abramson et al. 1989; Lavender and Watkins 2004; Verplanken et al. 2007; Takano and Tanno 2009). Accordingly, rumination has been associated with changes in FC and activity within regions of the DMN (Raichle et al. 2001). However to the best of our knowledge, no studies have yet investigated whether effects of affective stimulation on FC may be modulated by ruminative tendencies independent of depression, that is, in healthy subjects.

We used affective stimulation to investigate changes in brain network reconfiguration and their dynamic carry-over effects on subsequent resting states. To date, no previous study has integrated changes in neurobiological networks elicited by affective stimulation with concurrent physiological and psychological measures. Furthermore, until now, far too little attention has been paid to unravel carry-over effects of affective stimulation on the functional interplay between major ICNs. Previous investigations have employed mainly seed-based approaches, whereas changes on the level of networks have been largely neglected. Also, it is still unclear whether changes in brain network reconfiguration might be specific for affective and cognitive stimulation, respectively. To bridge these gaps, our experimental paradigm included fMRI scans both during and after affective stimulation with sad and neutral movies. These data were complemented with objective measures of HRV and subjective measures of mood state. In order to infer specificity of affective versus cognitive effects, we also investigated working memory tasks with two load levels. Using NBS with an underlying parcellation of major ICNs, we aimed to identify subnetworks associated with a changing psychological context. We hypothesized that, firstly, affective stimulation has a valence-dependent effect on both HRV and mood, secondly, that ICN patterns differ between affective and cognitive stimulation, and thirdly, that dynamic ICN configuration depends on valence-dependent carry-over effects. Furthermore, we tested whether the effect of affective stimulation on ICNs may be modulated by rumination.

Methods

Subjects

Twenty-two right-handed, healthy female subjects (aged 20–49 years, mean age 28.1 ± 6.5) completed the study. Subjects were recruited via local campus flyers and mailing lists. In addition to standard safety exclusion criteria for magnetic resonance imaging, subjects were screened for absence of any neurological or psychiatric disorders using the short version of the

Structured Clinical Interview for DSM-IV (SCID; (Wittchen et al. 1997). All subjects gave written informed consent and were reimbursed for participation. The study protocols were in accordance with the latest version of the Declaration of Helsinki and approved by the institutional review board of the Charité.

Experimental Paradigm

We adopted a rest-task-rest design on two consecutive days, each including either a cognitive or an affective task with two different valences (Fig. 1). As a general procedure on each day, the subjects first underwent a 10-min rs-fMRI scan, which served as a baseline. They then completed the task with one valence, followed by another 15-min rs-fMRI scan. Finally, they completed the task with the other valence, followed by a last 15-min rs-fMRI scan. The resting sessions following a task served to capture changes in intrinsic brain network connectivity patterns induced by the preceding task. During all rs-fMRI scans, subjects were instructed to keep their eyes closed, lie still, remain awake, and let their mind wander without explicitly engaging in any goal-directed tasks.

The sequence of the 2 tasks and the order of the affective and cognitive days were counterbalanced across subjects.

On the affective day, subjects were presented with 2 movies that had neutral and sad valence, each lasting 5 min. The sad movie was an excerpt from the film "21 Grams" directed by Alejandro González Iñárritu, which depicts a mother who loses her husband and both children in a hit-and-run accident. The same scene has been used in previous mood induction studies (Shiota et al. 2009; Hanich et al. 2014). The neutral movie was an excerpt from the film "The Son's Room" directed by Nanni Moretti and was selected because it has a similar domestic setting and also shows human faces. It depicts a daily scene in a family of 4 having dinner at home. Before watching each movie, subjects were presented with a short synopsis, which provided essential information about the characters and the plot unfolding before the scene. Subjects were instructed to watch the movies passively and refer themselves to the main character. Movies were shown in the dubbed German version. Black fade-ins and fade-outs as well as acoustic transitions were used to avoid an overly abrupt beginning and ending of the movie. Each movie was followed by a 15-min resting-state scan.

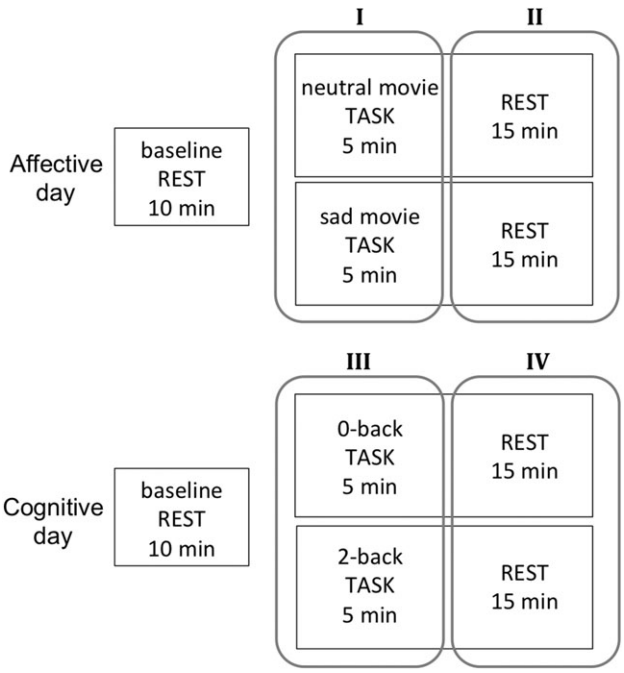

Figure 1. Experimental paradigm. Numbers indicate different analysis steps. I: Comparison of hf-HRV between sad and neutral movie. NBS was performed to identify a subnetwork that may be associated with a changing affective state between neutral movie and sad movie. II: NBS was performed to identify a subnetwork that may be associated with carry-over effects between rest after affective stimulations. Dynamic sliding-window analysis of selected NOIs was performed to compare temporal profile of FC strength between rest after affective stimulations. III: NBS was performed to identify a subnetwork that may be associated with a changing cognitive state between 0-back and 2-back working memory task. IV: NBS was performed to identify a subnetwork that may be associated with carry-over effects between rest after cognitive tasks. Dynamic sliding-window analysis of selected NOIs was performed to compare temporal profile of FC strength between cognitive tasks.

On the day of the cognitive task, subjects completed N-back tasks (Gärtner et al. 2014) with 2 different loads (i.e., 0-back and 2-back), each lasting 5 min. Each N-back task consisted of 7 blocks separated by short breaks of 9–15 s. In each block, a sequence of 15 digits (range: 1–4) was presented in a pseudo-randomized order. Digits were presented for 400 ms with an inter-stimulus-interval of 1400 ms. In the 0-back condition, subjects were asked to detect whether the digit shown on the screen was a "1". In the 2-back condition, subjects were asked to detect whether the current digit was identical to the one presented 2 trials back. Subjects were asked to respond as quickly and as accurately as possible by pressing a button using the right index finger. Before entering the scanner, they practiced both tasks until they reached an accuracy of 80% and no further improvement of performance was observed for 2 consecutive blocks. Subjects received no feedback on their task performance during the scanning. Each of the N-back tasks was followed by a 15-min resting-state scan.

Psychological Measures

After the scanning session on the affective day, subjects completed subjective ratings regarding their affective response to the movies on a 9-point Likert scale. The items were selected from Hanich et al. (2014) and include valence ("How happy/pleased or unhappy/dissatisfied are you?", 1 = very unhappy; 9 = very happy), arousal ("How awake/aroused or calm/drowsy do you feel?", 1 = very calm, 9 = very aroused), dominance ("How small/dominated/affected or secure/strong/confident do you feel?", 1 = very small, 9 = very strong), own affective experience ("How pleasant or unpleasant was your own experience of the scene?", 1 = very unpleasant, 9 = very pleasant) and own mood ("Did the movie influence your current mood?", 1 = very negative influence, 9 = very positive influence). To investigate the effect of affective valence on these subjective measures, paired *t*-tests were performed between sad and neutral movies ($N = 22$) and results are reported with Bonferroni correction for multiple comparisons.

The 23-item German version of the Response Style Questionnaire (RSQ-D) is designed to measure different coping styles by asking respondents what they generally do when they feel sad. The questionnaire consists of 2 scales: the rumination response scale (RRS), which consists of 15 items and can be subdivided into self-focused (7 items) and symptom-focused rumination (8 items), and the Distraction response scale (DRS), with 8 items (Bürger and Kühner, 2007). All items are rated on a 4-point Likert scale, ranging from 1, "almost never", to 4, "almost always." The RRS and DRS are reliable, independent of one another, have been shown to measure trait-like coping

styles and are not associated with, or confounded by, the state effects of depressed mood (Nolen-Hoeksema and Morrow 1991; Just and Alloy 1997).

Image Acquisition

Functional MRI images were acquired on a Siemens Trio 3 T scanner (Siemens, Erlangen, Germany) with a 12-channel radio-frequency (RF) head coil, using an T2*-weighted Echo Planar Imaging (EPI) sequence (37 axial slices of 3 mm thickness covering the whole brain, TR = 2000 ms, TE = 30 ms, 70° flip angle, 64 × 64 matrix, field of view = 192 × 192 mm^2, in-plane resolution = 3 × 3 mm^2). The baseline resting-state session consisted of 300 volumes, the resting-state sessions after task of 450 volumes and the task sessions of 147 volumes.

T1-weighted anatomical reference images were acquired using 3D-MPRAGE sequence (176 sagittal slices covering the whole brain, 1 × 1 × 1 mm^3 isotropic resolution, TR = 1900 ms, TE = 2.52 ms, 9° flip angle, 256 × 256 matrix). Participants were provided with earplugs to reduce scanner noise and subject motion was minimized using soft pads fitted between head and coil.

Physiological Recordings and Analysis

Electrocardiogram (ECG) was recorded via an electrode placed at the base of the back. This position is recommended to maximize the signal to noise of the R-peak in the ECG trace, as well as for subject comfort (Mullinger et al. 2013). Respiratory rhythm and volume were monitored using a pneumatic belt (Respiration Belt MR, Brain Products, Munich) strapped around the upper abdomen. Both ECG and respiratory data were recorded with a 100 Hz low-pass filtered and 5 kHz sampling rate, and were amplified with an MR-compatible EEG amplifier (BrainAmp ExG MR, Brain Products, Munich). ECG data was corrected for gradient artifacts using average artifact subtraction (Allen et al. 1998, 2000) implemented in Brain Vision Analyzer (Brain Products, Munich). The respiratory signal was low-pass filtered at 10 Hz to remove MR artifacts.

HRV was derived from ECG data during sad and neutral movies only and served as an objective control variable for potentially differing reactions to the movies. R-peaks of the ECG data were detected using Brain Vision Analyzer 2.0 (Brain Products, Munich) and inter-beat-intervals (IBIs) were calculated. HRV was analyzed in the frequency domain with the fast Fourier transform (FFT) algorithm implemented in Kubios 2.2 (Tarvainen et al. 2014). Relative power in the high frequency band (0.15–0.4 Hz; HF-HRV) was used as index for parasympathetic activity. Data of 3 subjects were excluded due to residual artifacts from head movement and gradient or long gaps in the acquisition.

To investigate the effect of affective valence on physiological measures, paired t-tests were performed between high-frequency HRV during sad and neutral movies ($N = 19$).

Image Preprocessing

Data were preprocessed using Matlab 2012b (The Mathworks Inc.), and the toolboxes SPM12, DPABI_V2.0, and DPARSFA_V4.0. The first 5 volumes were removed to account for signal equilibrium. To subtract the portion of cardiac pulsations and respiration from the global signal, we applied RETROICOR and RVHRCOR (Power et al. 2017). Specifically, time-locked cardiac and respiratory artifacts were reduced via RETROICOR (Glover et al. 2000), which performs slice-specific correction using a second-order Fourier expansion for both cardiac and respiratory regressors. RVHRCOR was applied to reduce low-frequency respiratory volume and heart rate artifacts (Chang and Glover 2009). Slice time correction was performed and data were realigned. The anatomical T1 images were coregistered to match the functional images, segmented and normalized using T1 unified segmentation. Nuisance covariates from white matter and cerebrospinal fluid as well as 6-rigid body realignment parameters and a first-order polynomial trend were regressed out prior to bandpass filtering (0.01–0.1 Hz). Correcting motion-related artifacts in fMRI data is essential, as they cause systematic, but spurious correlation patterns (Power et al. 2014; Burgess et al. 2016). Specifically, many long-distance correlations are decreased by subject motion, whereas many short-distance correlations are increased (Power et al. 2012a). Regression of the global signal was not performed, because its omission leads to higher test–retest reliability in graph metrics derived from rs-fMRI (Braun et al. 2012; Guo et al. 2012), which is particularly important for repeated measurements in the context of cognitive or affective challenges.

Data were scrubbed using Power's frame-wise displacement (FD) index with 0.5 as threshold (Power et al. 2012). Volumes exceeding this threshold were deleted together with 1 preceding and 2 following timepoints, because the BOLD signal change created by motion is most likely not restricted to one TR. Values of these timepoints were interpolated using cubic spline method, because we calculated dynamic FC and therefore needed to maintain the number of timepoints. We noticed that when a volume to be scrubbed occurred at the beginning or end of the timeseries, the interpolation algorithm introduces an artificially high value. To correct this, the affected timeseries were firstly patched at the beginning or the end with one or three replicates of the first or last volume, respectively. Second, the FD indices for the artificially introduced volumes were set to zero. Then, scrubbing was performed on the patched timeseries and the artificially introduced volume patches were removed. We used unsmoothed data for timeseries extraction.

Two subjects were excluded for the cognitive day due to incomplete data in the rest after task session. Three subjects were excluded for the affective day due to excessive head motion (i.e., they either exceeded head motion by 3.0 mm or 3.0°, at a 3 mm isotropic voxel size, or more than 50% of their the timeseries were interpolated during scrubbing). As a result, data of 19 (age: 28.1 ± 6.5) and 20 (age: 28.3 ± 6.8) subjects were usable for analysis of the affective and cognitive day, respectively.

fMRI Data Analysis

To analyze changes in connectivity patterns between the experimental conditions, the brain was modeled as a network and analyzed with methods of graph theory. This network consisted of nodes (brain regions) that are interconnected by edges (measures of FC).

Forty-two spherical nodes were placed in the DMN, the DAN, and the CEN. This parcellation has been developed by Spreng et al. 2013 using datasets from three independent studies that included autobiographical planning, visuospatial planning, and counting tasks with the aim to obtain an functional parcellation defined by significant and reliable task-based regional activations. Therefore, network maps were derived from statistically significant activation maps for each ICN from a group analysis of each of the three independent studies using

multivariate spatiotemporal partial least squares technique, which identifies whole-brain patterns of covariance. Network maps representing the spatial overlap of significant activity within these networks were computed. Each network node comprised a 5 mm radius sphere centered on the mean peak maxima of the network map. Nodes were further refined to ensure spatial demarcation and to preserve integrity of anatomical boundaries (Spreng et al. 2013).

Because subregions of the PCC are functionally distinct, we added 2 unilateral spheres in dorsal PCC (assigned to CEN) and two unilateral spheres in ventral PCC (assigned to DMN) with a radius of 6 mm each (see Leech et al. 2011). A list of nodes, coordinates, and network affiliation is provided in Supplementary Table S1. Our parcellation consisted of 19 DMN nodes (12 left, 7 right hemisphere), 10 DAN nodes (5 left, 5 right), and 17 CEN nodes (8 left, 9 right) (Fig. 2). Extracted time courses of these regions were pair-wise correlated and Pearson correlation coefficients representing a measure of FC were entered in a square correlation matrix per subject.

To identify connections that may be associated with a changing psychological context, a method called NBS was applied. Specifically, subnetworks identified using a t-statistic represent a subset of nodes sharing altered functionally connected edges, which, as a whole, are statistically unlikely to be due to random chance. The resulting subnetwork is statistically significant at a family wise error (FWE) corrected value of $P < 0.05$. However, the influence of individual components cannot be identified. The NBS technique has been described in detail by (Zalesky and Breakspear 2010).

Although the subnetworks need to be considered as a whole, altering the arbitrarily chosen primary t-statistic threshold can vary the extent of the subnetwork. We tested a range of t-thresholds between 2.0 and 5.0 in steps of 0.2. It should be noted that decreasing the threshold creates a larger subnetwork and a smaller subnetwork found with a higher t-threshold would usually be encompassed inside the larger one. Therefore, when using NBS to compare experimental conditions, we report subnetworks that may have been derived from unequal t-thesholds, but were comparable in size.

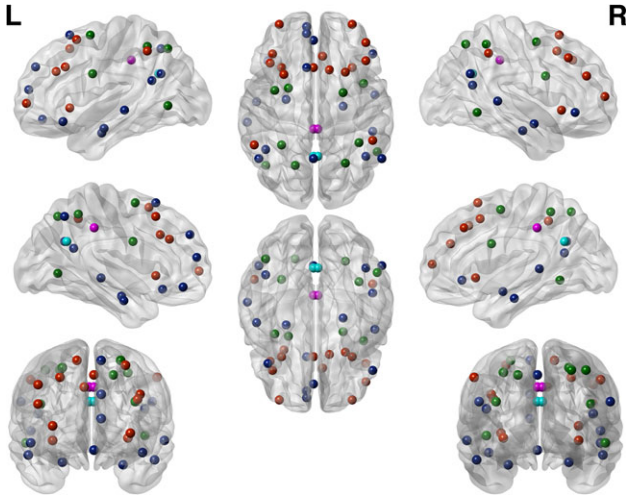

Figure 2. ICN parcellation consists of 19 DMN nodes (blue spheres, 12 left, 7 right hemisphere), 10 DAN nodes (green spheres, 5 left, 5 right), 17 CEN nodes (red spheres, 8 left, 9 right), visualized using BrainNet Viewer (http://www.nitrc.org/projects/bnv/) (Xia et al. 2013).

Static NBS was used to identify clusters of altered connections specific to affective movies and cognitive tasks. For each experimental day, one statistical model was set up and included a total of 5 conditions (baseline, 2 affective movies (or N-back tasks), as well as the two rest- periods after affective movie (or cognitive task)).

Firstly, NBS was performed to identify subnetworks that are stronger/weaker connected in the neutral movie condition than the sad movie condition and vice versa.

Strength of a NBS subnetwork was calculated by adding FC values of the respective connections.

Secondly, dynamic NBS was used to assess temporal variability of carry-over effects on the two rest after movie (or cognitive task) conditions. Therefore, time courses of all nodes were cut into 3 nonoverlapping intervals and 1 statistical model was created separately for each interval and in the same way as for the static version. Resting-state data were cut into intervals with a duration of 3 minutes (90 TR) each. Network nodes that mediated most of the connectivity changes in the contrast *rest after sad movie versus rest after neutral movie* were identified as nodes-of-interest (NOIs).

To further explore the dynamic changes in FC after the movies, sum nodal strength of each NOI was calculated in a sliding-window manner for resting-state after movies, using 60 s windows with 50% overlap between adjacent windows. Cognitive states have been shown to be correctly identified using windows of 30–60 seconds (Shirer et al. 2012) and thus we chose a longer window size to allow for a robust estimation of covariance structure and to capture potential transition states with high signal-to-noise ratio. To identify the increase or decrease tendency of the nodal strength in each interval, sliding-window nodal strength was calculated with 40 s windows with 75% overlap, and correlated with time. The slope of this linear fitting represented the increase or decrease tendency of the nodal strength in the corresponding interval. To obtain a fine-grained slope profile, we increased the number of data points by reducing the window length and increased their overlap. Brain network topology was found to stabilize at window lengths of 30 s (Jones et al. 2012), but we chose a slightly longer window length to include a buffer.

We examined the significance of each slope and applied Bonferroni correction (*P*-value indicated by p_B). To examine the difference in slopes between 2 conditions (i.e., rest after neutral movie and rest after sad movie), we applied hierarchical multiple regressions (HMR) using time, condition, and time × condition as predictors. Significant time × condition interactions indicated that the increase or decrease tendency (slopes) differed between rest after neutral and rest after sad. The *P*-values in the HMRs were also Bonferroni-corrected.

To probe the relationship between trait rumination and carry-over effects, nodal strength of each NOI in each interval was summed up and correlated with the three subscales of the RSQ-D.

Results

Behavioral and Physiological Effects of Affective Stimulation

Compared with the neutral movie, paired *t*-tests showed that the sad movie was rated as both more negative ($t(21) = -6.67$, $p_B < 0.001$) and arousing ($t(21) = 6.08$, $p_B < 0.001$). After watching the sad movie, subjects felt less in control (i.e., reduced dominance, $t(21) = -3.58$, $p_B = 0.0089$) and experienced more

Figure 3. (*A*) Subjective ratings on affective responses to the neutral and sad movies plotted in blue and red, respectively. The whiskers represent standard deviation. *P*-values were Bonferroni-corrected for five comparisons (indicated by p_B): $^{***}p_B < 0.001$, $^{**}p_B < 0.01$. (*B*) Decrease of high-frequency HRV during affective stimulation with negative valence (sad movie); $^{*}P < 0.05$.

negative emotions ($t(21) = -3.55$, $p_B = 0.0095$) as well as subdued mood ($t(21) = 6.08$, $p_B = 0.0028$, Fig. 3A).

Concerning HRV, data shows a decrease in relative power in high frequency band while watching the sad movie compared to watching the neutral movie ($t(18) = -2.54$, $P = 0.0204$, Fig. 3B), which represents a downregulation of the PNS upon affective stimulation with negative valence.

fMRI NBS Findings

Valence-Dependent Brain Network Changes During Affective Stimulation

Using static NBS, different networks of connections associated with distinct affective valence were found when considering the contrasts *neutral movie > sad movie* and *neutral movie < sad movie* (Supplementary Table S2).

For each contrast, a significant network with comparable sizes across both contrasts was selected and henceforth termed "subnetwork".

The seven regions involved in the subnetwork showing increased FC in the sad movie compared to the neutral movie at t-threshold 3.2 ($P = 0.007$) were: left superior temporal sulcus, bilateral posterior inferior parietal lobule, bilateral anterior temporal lobe, right middle frontal gyrus (Brodmann area 6), and right inferior precentral sulcus (Table 1, Supplementary Figure S1A). Overall, mainly inter-CEN-DMN connections were upregulated during sad compared to neutral movie (Fig. 4A).

The 8 regions involved in the subnetwork showing reduced FC in the sad movie compared to the neutral movie condition at t-threshold 2.8 ($P = 0.046$) were bilateral posterior inferior parietal lobule, bilateral inferior frontal gyrus, left dorsomedial prefrontal cortex, left anterior insula, left middle frontal gyrus (Brodmann area 9), right frontal eye field, and left rostrolateral prefrontal cortex (Table 1, Supplementary Figure S1B). Mainly intra-DMN connections were downregulated during sad compared to neutral movie (Fig. 4B).

Load-Dependent Brain Network Changes During Cognitive Tasks

To investigate specificity of our findings regarding the effect of affective stimulation on brain network changes, we next focused on respective changes induced by cognitive tasks.

Using static NBS, different networks of connections associated with distinct cognitive load were found when considering the contrasts 0-back < 2-back and 0-back > 2-back (Supplementary Table S3).

Table 1. Undirected connections of the NBS subnetwork of the two contrasts *neutral < sad* (t = 3.2, 7 edges, 8 nodes) and *neutral > sad* (t = 2.8, 8 edges, 9 nodes). Nodes are color-coded by ICN affiliation (blue = DMN, red = CEN, green = DAN). For abbreviations see Supplementary Table S1.

	neutral < sad, t = 3.2	
STS_l	-	aTL_r
STS_l	-	MFG(BA6)_r
pIPL_l	-	MFG(BA6)_r
pIPL_r	-	MFG(BA6)_r
aTL_l	-	MFG(BA6)_r
aTL_l	-	dlPFC_l
pIPL_l	-	iPCS_r
	neutral > sad, t = 2.8	
pIPL_l	-	pIPL_r
pIPL_l	-	dmPFC_l
pIPL_l	-	IFG_l
IFG_r	-	IFG_l
MFG(BA9)_l	-	IFG_l
rlPFC_l	-	pIPL_r
MFG(BA9)_l	-	FEF_r
aINS_l	-	FEF_r

For each contrast, significant subnetwork(s) with comparable sizes across both contrasts were selected. For the contrast *0-back < 2-back*, the subnetwork at t-threshold 3.8 was comprised of two networks that were not interconnected. The 8 regions involved in the first of these networks showing increased FC in the 2-back task ($P < 0.001$) were bilateral frontal eye field, right superior orbital gyrus, left inferior precentral sulcus, left precuneus, right rostrolateral prefrontal cortex, right middle frontal gyrus (Brodmann area 6), and right anterior insula (Table 2, Supplementary Figure S2A).

Mainly inter-CEN-DAN connections were upregulated during 2-back compared to 0-back task. The 4 regions involved in the second network ($P < 0.001$) were left superior parietal lobule, left dorsolateral prefrontal cortex, left middle frontal gyrus (Brodmann area 9), and left medial superior prefrontal cortex (Table 2, Supplementary Figure S2A).

Mainly intra-CEN connections were downregulated during 2-back compared to 0-back task. The 9 regions involved in the subnetwork showing reduced FC in the 2-back compared to the 0-back condition (t-threshold=3.8, $P < 0.001$) were: bilateral dorsal posterior cingulate cortex, bilateral middle frontal gyrus

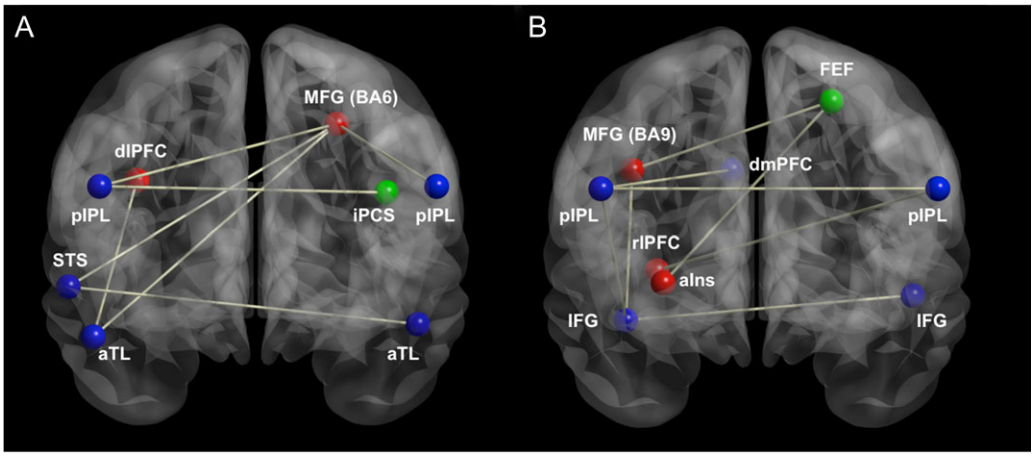

Figure 4. Brain network of the contrast (*A*) *neutral* < *sad* (t = 3.2, 7 edges, 8 nodes) and (*B*) *neutral* > *sad* (t = 2.8, 8 edges, 9 nodes) in neurological orientation and visualized using BrainNet Viewer (http://www.nitrc.org/projects/bnv/) (Xia et al. 2013). Nodes are color-coded by ICN affiliation (blue = DMN, red = CEN, green = DAN).

(Brodmann area 6), left middle frontal gyrus (Brodmann area 9), left medial superior prefrontal cortex, left inferior frontal gyrus, right posterior inferior parietal lobule, and right ventral posterior cingulate cortex (Table 2, Supplementary Figure S2B).

Valence-Dependent Brain Network Changes after Affective Stimulation

Using dynamic NBS, different networks of connections associated with carry-over effects after affective stimulation were found when considering the contrast *rest after neutral movie* < *rest after sad movie* in window 2 and in window 3 (Supplementary Table S4). For the reverse contrast, there were no significant results.

For the contrast *rest after neutral* < *rest after sad*, subnetworks with comparable sizes across both windows were selected. For window 2, the subnetwork showing increased FC in the rest after sad condition (*t*-threshold=2.6, $P < 0.044$) contains fourteen regions: bilateral dorsolateral prefrontal cortex (dlPFC), left medial superior prefrontal cortex, left middle frontal gyrus (Brodmann area 9), left frontal eye field, left superior occipital gyrus, left inferior precentral sulcus, left inferior frontal gyrus, left superior frontal gyrus, left precuneus, left superior temporal sulcus, left posterior inferior parietal lobule, left ventral medial prefrontal cortex, and right hippocampal formation (Table 3, Fig. 5A). Importantly, left dlPFC connects to all 3 major ICN.

For window 3, the subnetwork showing increased FC in the rest after sad condition (t-threshold = 3.2, $P = 0.005$) contains eleven regions: left dorsal posterior cingulate cortex (dPCC), bilateral superior occipital gyrus, right superior parietal lobule, left middle frontal gyrus (Brodmann area 6), left posterior inferior parietal lobule, left superior temporal sulcus, right inferior frontal gyrus, left precuneus, left anterior temporal lobe, and right hippocampal formation (Table 3, Fig. 5B). In this subnetwork, the left dPCC is the only CEN node.

Dynamic Connectivity Strength of Selected Regions

Since both left DLPFC and left dPCC mediated most of the valence-dependent carry-over effects of affective stimulation, these 2 regions were identified as nodes-of-interest (NOIs). To further explore dynamic changes in connectivity strength of the NOIs after affective stimulation, sum nodal strength was calculated in a sliding-window manner for the 15-min resting-state scans after each affective stimulation (window-size = 30 TR, with 50% overlap).

Compared with rest after neutral movie, left DLPFC showed more positive nodal strength in rest after sad movie at an earlier stage (90–180 TRs, see Fig. 6A); whilst left dPCC showed more positive nodal strength in rest after sad movie at a later stage (181 to 270 TRs, see Fig. 6B). In contrast, similar sliding-window analysis for resting-state scans after 0-back and 2-back tasks showed no significant difference in nodal strength in these two regions (Fig. 6C and D).

To investigate the inclinations of dynamic connectivity changes in both left DLPFC and left dPCC after affective

Table 2. Undirected connections of the NBS subnetworks of the 2 contrasts *0-back* < *2-back* (t = 3.8, first network: 7 edges, 8 nodes, second network: 3 edges, 4 nodes) and *0-back* > *2-back* (t = 3.8, 10 edges, nine nodes).

	0back < *2back*, *t* = 3.8	
FEF_l	-	**SOG_r**
FEF_r	-	SOG_r
FEF_r	-	rlPFC_r
SOG_r	-	aINS_r
SOG_r	-	MFG(BA6)_r
iPCS_l	-	rlPFC_r
Prec_l	-	aINS_r
	0back < *2back*, *t* = 3.8	
SPL_l	-	dlPFC_l
SPL_l	-	msPFC_l
SPL_l	-	MFG(BA6)_l
	0back > *2back*, *t* = 3.8	
dPCC_r	-	MFG(BA6)_r
dPCC_r	-	MFG(BA6)_l
dPCC_r	-	MFG(BA9)_l
dPCC_r	-	**msPFC_l**
dPCC_l	-	MFG(BA6)_r
dPCC_l	-	MFG(BA9)_l
dPCC_l	-	msPFC_l
IFG_l	-	msPFC_l
pIPL_r	-	MFG(BA9)_l
vPCC_r	-	MFG(BA9)_l

Nodes are color-coded by ICN affiliation (blue = DMN, red = CEN, green = DAN). For abbreviations see Supplementary Table S1.

stimulation, dynamic sliding-window analysis was performed again with 20 TR window-size and 75% overlap (Fig. 7). For 5 different windows during resting-state scans after affective stimulation, averaged nodal strength of the NOI was regressed against time (for detailed statistics, see Supplementary Table S5).

Table 3. Undirected connections of the NBS subnetwork of the contrasts *rest after neutral* < *rest after sad* for window 2 (t = 2.6, *P* = 0.004, 14 edges, 14 nodes) and window 3 (*t* = 3.2, *P* = 0.005, 10 edges, 11 nodes).

	rest_neutral < rest_sad **window 2, *t* = 2.6, *P* = 0.044**	
IFG_l	-	pIPL_l
SFG_l	-	HF_r
Prec_l	-	iPCS_l
STS_l	-	iPCS_l
pIPL_l	-	dlPFC_r
STS_l	-	dlPFC_r
STS_l	-	dlPFC_l
vmPFC_l	-	dlPFC_l
HF_r	-	msPFC_l
Prec_l	-	msPFC_l
FEF_l	-	dlPFC_l
SOG_l	-	dlPFC_l
FEF_l	-	MFG(BA9)_l
dlPFC_l	-	msPFC_l
	rest_neutral < rest_sad **window 3, *t* = 3.2, *P* = 0.005**	
pIPL_l	-	STS_l
STS_l	-	HF_r
IFG_r	-	MFG(BA6)_l
Prec_l	-	SPL_r
SOG_l	-	MFG(BA6)_l
SOG_r	-	MFG(BA6)_l
SPL_r	-	MFG(BA6)_l
aTL_l	-	dPCC_l
pIPL_l	-	dPCC_l
Prec_l	-	dPCC_l

Nodes are color-coded by ICN affiliation (blue = DMN, red = CEN, green = DAN). For abbreviations see Supplementary Table S1.

The nodal strength of left DLPFC increased from 1 to 180 TRs during rest after sad movie (p_B = 0.006 and 0.0145, respectively), and decreased between 181 and 270 TRs (p_B < 0.001). In contrast, in rest after neutral movie, nodal strength of left DLPFC decreased earlier (91–180 TRs, p_B = 0.0175; see Fig. 7A).

The nodal strength of left dPCC increased from 1 to 90 TRs during rest after sad movie (p_B = 0.0015), and decreased from 181 to 270 TRs (p_B = 0.011). In contrast, in rest after neutral movie nodal strength of left dPCC increased from 1 to 90 TRs (p_B = 0.0015), decreased both between 91 and 180 TRs (p_B = 0.0215) and between 361 and 455 TRs (p_B = 0.016; see Fig. 7B). p_B indicates *P*-value of the slope after Bonferroni correction.

We compared the difference in slopes between rest after neutral and rest after sad conditions using hierarchical linear regression. Differences in slopes were significant from 91 to 180 TRs and from 180 to 270 TRs (see Supplementary Table S6)

Region-Specific Correlation Between Dynamic Carry-Over Effects After Affective Stimulation and Rumination

To examine the association between dynamic carry-over effects after affective stimulation and trait rumination, dynamic nodal strength of left DLPFC and left dPCC were correlated with scores on 3 subscales of the RSQ (symptom-related rumination 15.53 ± 3.88; self-related rumination 14.11 ± 3.02; distraction 19.95 ± 4.55). At the early stage, during rest after sad movie (1–90 TRs), there was a significant increase in nodal strength of left DLPFC (Supplementary Table S5 and Fig. 7A). This increase in left DLPFC nodal strength correlated positively with the symptom-related rumination score ($r(18)$ = 0.470, *P* = 0.042), whilst the same correlation did not reach significance for rest after neutral movie at the early stage (see Table 4). At the second stage (91–180 TRs), the nodal strength of left DLPFC continued to increase during rest after sad movie, while it started to decrease during rest after neutral movie (Supplementary

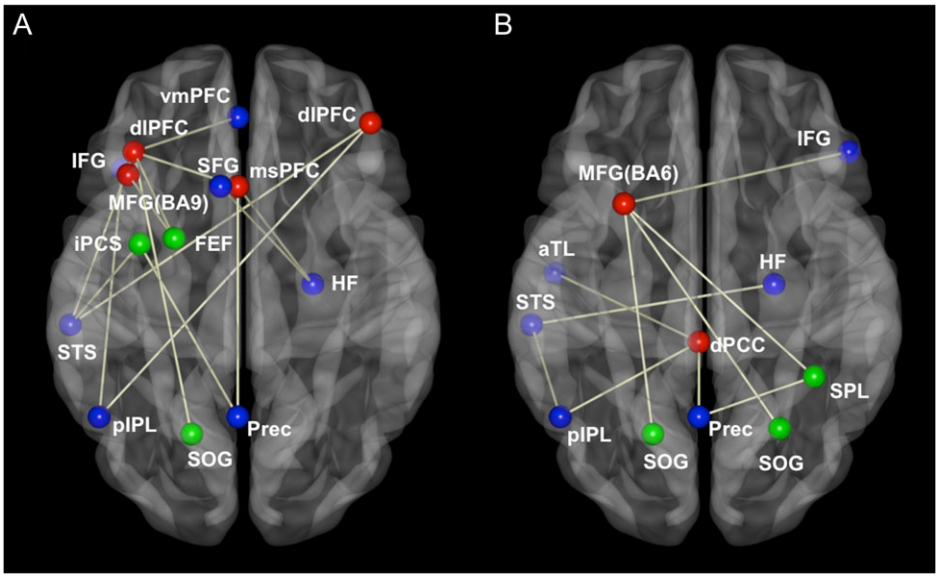

Figure 5. Brain network of the contrast (*A*) rest after neutral < rest after sad in window 2 (*t* = 2.6, 14 edges, 14 nodes) and (*B*) rest after neutral < rest after sad in window 3 (*t* = 3.2, 10 edges, 11 nodes) in neurological orientation and visualized using BrainNet Viewer (http://www.nitrc.org/projects/bnv/) (Xia et al. 2013). Nodes are color-coded by ICN affiliation (blue = DMN, red = CEN, green = DAN).

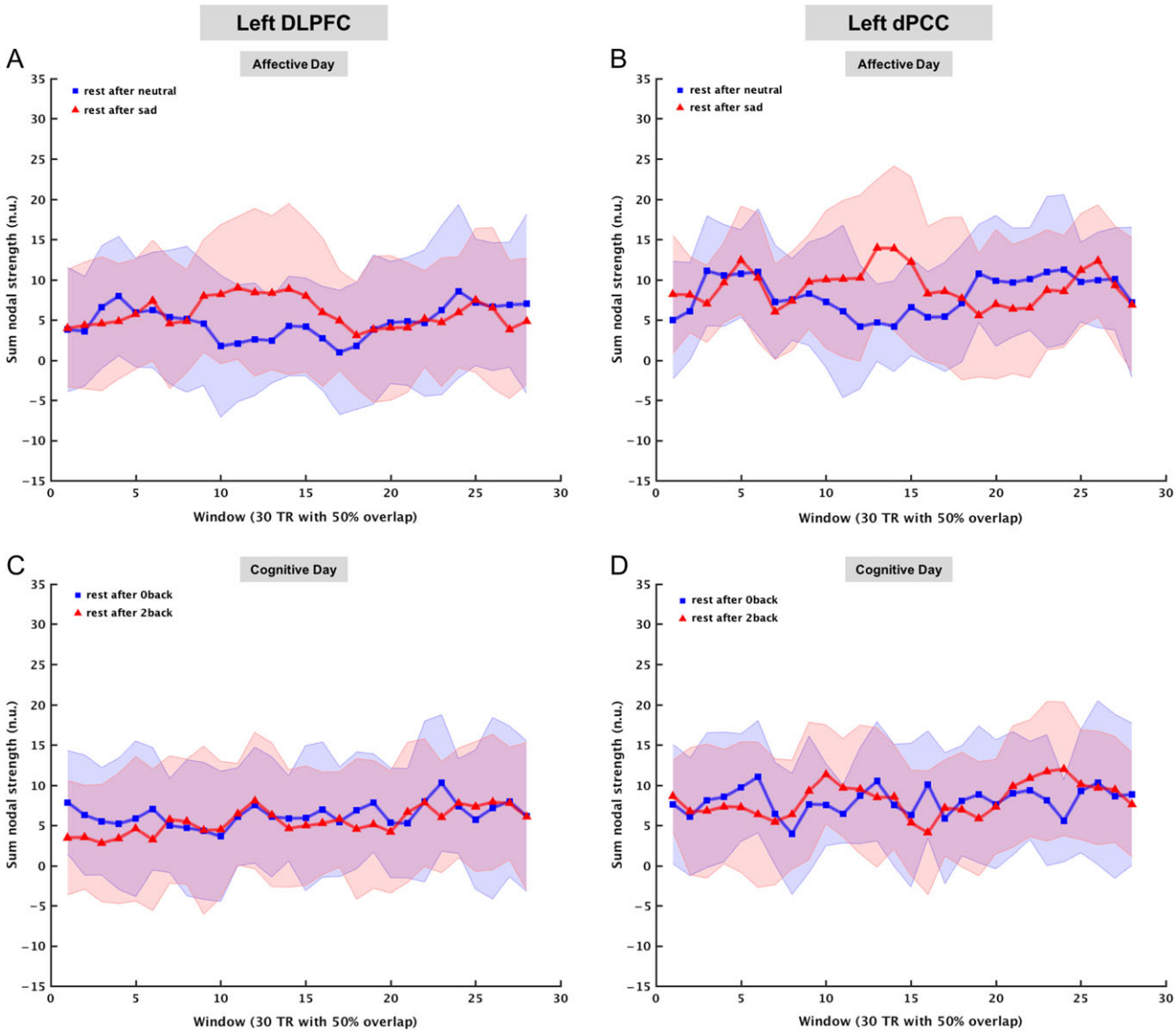

Figure 6. Dynamic sliding-window analysis (window length: 30 TR = 60 s, 50% overlap) of connectivity strength measured as sum of nodal strength in (*A*) left DLPFC and (*B*) left dPCC during rest after neutral movie (blue squares) and rest after sad movie (red triangles). Dynamic sliding-window analysis with the same parameter was also performed for (*C*) left DLPFC and (*D*) left dPCC during rest after 0-back task (blue spheres) and rest after 2-back task (red triangles).

Table S5 and Fig. 7*A*). Left DLPFC nodal strength during this stage correlated positively with symptom-related rumination scores for both conditions (rest after sad movie: $r(18) = 0.615$, $P = 0.005$; rest after neutral movie: $r(18) = 0.575$, $P = 0.010$; see Table 4).

No significant correlation was found for nodal strength in left dPCC at any stage.

Discussion

Our study aimed to integrate changes in neurobiological networks elicited by affective stimulation with concurrent physiological and psychological measures. Results show that affective stimulation with a sad movie impacts not only mood and HRV, but also induces valence-dependent brain network changes that were specific for affective stimulation. After affective stimulation with negative valence, brain networks including left dlPFC and left dPCC temporarily increased their connectivity strength. These valence-specific dynamic carry-over effects showed a region-specific correlation with rumination in dlPFC.

Behavioral and Physiological Effects of Affective Stimulation

Regarding effects of affective stimulation on psychological and physiological states, we observed that the sad movie clip was experienced as more negative, arousing, and overwhelming than the neutral movie (Fig. 3*A*). Furthermore, the sad movie induced decreases in high-frequency HRV (Fig. 3*B*), which represent a downregulated parasympathetic system that constitutes a nonphysiological stress state and has been linked to the development of heart disease (Montano et al. 2009) and depression (Licht et al. 2008; Kemp et al. 2010). These valence-dependent effects during affective stimulation on mood and HRV validate the diverging influence of the 2 movies.

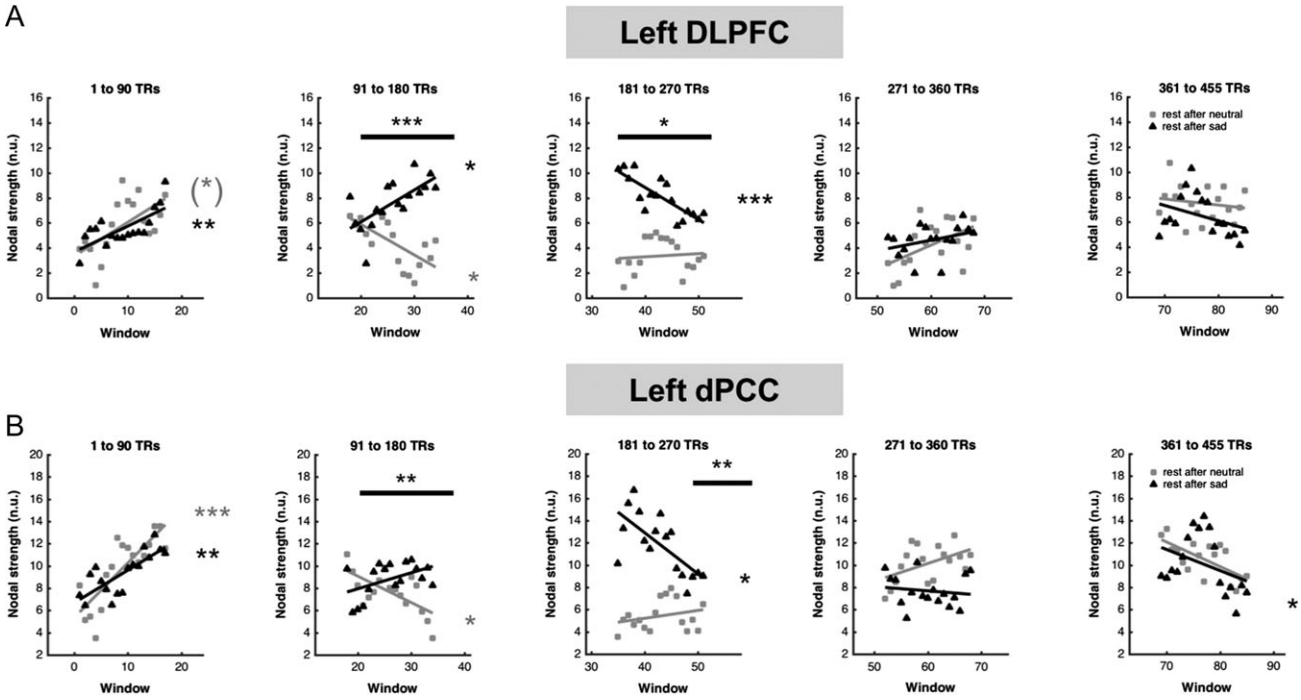

Figure 7. Temporal differences between windowed (window length: 20 TR = 40 s, 75% overlap) FC strength measured as average of nodal strength between rest after neutral movie (gray squares) and rest after sad movie (black triangles) in (*A*) left dlPFC and (*B*) left dPCC. Linear regression lines visualizes slope of nodal strength during each window. *P*-value of each slope was Bonferroni-corrected for multiple comparisons (indicated by p_B) and indicated by color-coded stars (black: rest after sad movie, gray: rest after neutral movie), where $^{***}p_B < 0.001$, $^{**}p_B < 0.01$, $^{*}p_B < 0.05$, and (*) indicates marginal significance: $p_B < 0.06$. Differences between regression slopes were examined by hierarchical linear regression and significant differences in slopes between the two conditions are marked with a horizontal black bar where $^{***}p_B < 0.001$, $^{**}p_B < 0.01$, $^{*}p_B < 0.01$. For detailed statistics of the regression models, please see Supplementary Tables S5 and S6.

Table 4. Results of Pearson's Correlation analyses between subscales of the RSQ-D and nodal sum strength in left dlPFC.

		Sum nodal strength in left DLPFC				
		1–90 TRs	91–180 TRs	181–270 TRs	271–360 TRs	361–455 TRs
Rest after sad movie						
Symptom-related Rumination	*r*	0.470*	0.615**	0.252	0.332	0.195
	P	0.042	0.005	0.297	0.164	0.423
Self-related Rumination	*r*	−0.262	0.084	0.181	0.073	−0.166
	P	0.279	0.733	0.458	0.767	0.498
Distraction	*r*	0.248	−0.187	0.016	0.075	0.133
	P	0.306	0.444	0.948	0.759	0.587
Rest after neutral movie						
Symptom-related Rumination	*r*	0.420	0.575**	0.162	−0.021	−0.078
	P	0.073	0.010	0.509	0.932	0.751
Self-related Rumination	*r*	−0.018	−0.017	−0.295	0.002	−0.131
	P	0.943	0.946	0.221	0.995	0.593
Distraction	*r*	0.025	−0.103	0.164	0.441	0.369
	P	0.918	0.675	0.502	0.059	0.120

Number of subjects=19, df = 17, window length = 90 TR, 0 % overlap, **: $P < 0.01$, *: $P < 0.05$.

Brain Network Changes During Affective Stimulation are Valence-dependent

Moreover, we observed valence-dependent brain network changes during affective stimulation in the sense that during the sad movie predominantly inter-CEN-DMN connections were upregulated, while predominantly intra-DMN connections were downregulated compared to the neutral movie (Fig. 4, Table 1). Our finding corroborates evidence from a previous study, which demonstrated that viewing a negative film clip is associated with increases in effective connectivity between DMN and CEN (Hyett et al. 2015). The reported valence-dependent brain network changes during affective stimulation involved connectivity changes to regions like dmPFC, dlPFC, and insula, whose activation has been robustly associated with affective processing (Lindquist et al. 2012). The DMN regions STS and IFG are part of NBS subnetworks found in our study and have previously been reported to belong to higher-order association areas, which respond to naturalistic audiovisual

stimuli (Hasson et al. 2004). However, the observed valence-dependent effect also involved regions in the DMN, such as pIPL, which are associated with information integration and involved in global control of multiple functional domains (Igelström and Graziano 2017). Thus, our study expands findings of previous seed-based studies on affective stimulation, which only focused on brain regions activated in affective tasks.

During cognitive stimulation, higher cognitive load (*2-back* vs. *0-back*) was mainly associated with increased inter-CEN-DAN connections and decreased intra-CEN connections (Table 2).

Previously, reconfigurations of frontoparietal and frontotemporal networks with altered interactions between modules were found upon effortful working memory challenges (Braun et al. 2015). Comparing the results of the present study and Braun et al. there is an overlap in that medial frontal regions and left dlPFC seem to be more active in low and high N-back task loads, respectively.

Valence-Dependent Carry-Over Effects after Affective Stimulation

Carry-over effects occur when an early experimental condition influences a later one. For example, an influence of prior cognitive or affective stimulation may linger in the subject's mind and its aftermath can be reflected in subsequent temporal connectivity profiles of brain areas as carry-over effects (Barnes et al. 2009). The here reported temporary increase in connectivity strength after the sad movie in brain networks that include nodes in left dlPFC and left dPCC indicates a valence-specific dynamic carry-over effect (Fig. 5, Table 3). The dlPFC is activated during stimulus evaluation and mental states, in which participants attend to affective feelings or perceptions (i.e., holding affective information in mind in order to categorize it, Lindquist et al. 2012). The PCC is related to storing representations of prior experiences, in order to make meaning of core affective inputs that come either from the self or from observing affective responses of others (Lindquist et al. 2012).

Carry-over effects in resting-state after higher cognitive load involved mainly decreased intra-CEN and inter-CEN-DMN connections, which did not overlap with those of the valence-specific carry-over effect found in resting-state after the sad movie. Our results extend previous findings of reconfiguration of frontal brain networks during an executive control task (Braun et al. 2015) and support a valence-specific network reconfiguration between CEN and DMN, especially mediated by left dlPFC and left dPCC. Carry-over effects of joy and fearful movies on PCC connectivity have been investigated, however, the difference between the 2 tested emotions was not significant (Eryilmaz et al. 2011). This discrepancy with our findings may be explained by the distinct emotions displayed in the respective movies as well as by the fact that these emotions most likely also differed with regard to arousal.

Moreover, we found that carry-over effects on nodal strength in the two NOIs were firstly task-specific, since the observed differences after affective stimulation were absent after cognitive tasks (Fig. 6). Second, the increases in nodal strength of the 2 NOIs were valence-specific, because they were only observed after watching the sad movie (Fig. 6*A*,*B*). Third, carry-over effects on nodal strength were region-specific, because left dlPFC and left dPCC were characterized by distinct temporal pace (Fig. 7).

In left dlPFC, nodal FC strength steeply increased during minutes 3–6 and steeply decreased during minutes 6–9 in the rest after sad condition, whereas in the rest after neutral condition it decreased only during minutes 3 and 6 (Fig. 7*A*). In left dPCC, nodal FC strength slowly increased during minutes 1–3, remained on a plateau until it steeply decreased during minutes 6–9 in the rest after sad condition, whereas in the rest after neutral condition it steeply increased during minutes 3–6 and decreased during minutes 6–9 (Fig. 7*A*). The valence-specific increase in nodal strength after the sad movie illustrates a more intensive carry-over effect, which entails a delayed disturbance of network connectivity patterns and consequently a delayed recovery to baseline levels. The observed carry-over effect was not present immediately at the start of the resting-state after the sad movie. Instead, temporal dynamics after watching the sad movie were most pronounced between minutes 3.5–11 after the end of the sad movie.

To date, there is only little published data on carry-over effects. Previous investigations based on cognitive tasks revealed that the intensity of carry-over effects depends on the difficulty or impact of the preceding task (Barnes et al. 2009). Accordingly, acute social stress induced strengthened thalamocortical connectivity and weakened cross-hemispheral parietotemporal connectivity (Maron-Katz et al. 2016). Moreover, investigating long-term carry-over effects, it has been shown that one hour after a psychosocial stress task resting-state FC between amygdala and vPCC was increased (Veer et al. 2011) and 90 min after a stressful arousing experience the recovery pattern of DMN FC had returned to prestress levels (Vaisvaser et al. 2013). Evidence from a rest-task-rest study that presented stimuli with socio-affective content showed that carry-over effects were most pronounced after stimuli with negative valence (Borchardt et al. 2015). Taken together, we assume that the prominent carry-over effect after sad movie can be explained by the distressing impact of the content of the sad movie.

A region-specific correlation between dynamic carry-over effects after affective stimulation in a CEN node and rumination style was found: the stronger the dynamic connectivity strength of left dlPFC, the higher the symptom-related rumination (Table 4). Abnormal patterns of fluctuating communication among brain networks involved in regulating self-referential thinking have been associated with ruminative thinking and depression: Higher resting-state DMN activity compared to activity in a task-positive network has been related to higher levels of maladaptive rumination in MDD patients (Hamilton et al. 2011). Furthermore, increased dynamic FC between mPFC (part of DMN) and insula (part of CEN) has been related to higher levels of rumination in MDD (Kaiser et al. 2015). Ruminative tendencies are considered trait-like characteristics and increase the risk to develop depressive disorders (Just and Alloy 1997; Nolan et al. 1998; Kuehner and Weber 1999; Nolen-Hoeksema and Davis 1999). One might speculate, that in subjects with higher ruminative tendencies, the negative affective stimulation activated mood-congruent representations and persisting negative thoughts, which are reflected in prolonged carry-over effects following affective stimulation. Underscoring the role of increased resting-state activity within the DMN for emergence and maintenance of negative mood states are findings showing an attenuation of DMN activity in MDD patients with remission after treatment (Anand et al. 2005). Therefore, our findings imply that connectivity strength of dlPFC modulates ruminative thinking after affective stimulation. To investigate whether prolonged carry-over effects after affective stimulation could be marker for depression

vulnerability, prospective longitudinal studies in healthy subjects as well as studies in MDD patients would be the crucial next step.

Limitations

The inclusion of only female subjects may be seen as a weak point of this study. Imporantly, regions like the amygdalae, the IFG, and the PCC have been shown to activate differently in males and females during emotional processing (Schulte-Rüther et al. 2008; Fine et al. 2009). Hofer et al. (2007) investigated sex differences in neural activation associated with exposure to positive and negative emotional picture stimuli and demonstrated greater PCC activation for negative and positive stimuli in females, who also reported a stronger negative impact on mood during stimulation with negative valence. Based on these results, we expected greater carry-over effects in females.

Generally, we opted for inclusion of as many usable datasets as possible to increase statistical power. Therefore, the number of subjects differs slightly between the analyses.

The use of naturalistic film viewing with affective content offers a realistic paradigm to investigate emotional processing and has been validated by Hasson et al. 2004.

Since the current results focus on task-specific effects of the paradigm, general effects have not been considered yet, but deserve separate attention and are thus currently analyzed.

Data from the 2 experimental days were considered as independent datasets and thus analyzed separately. Nevertheless, the respective results were descriptively compared with each other.

Future studies should also include affective stimulation with positive valence in order to investigate whether the here reported effects on FC are specific for negative affective stimulation or rather reflect the impact of affective stimulation per se.

Affective stimulation and cognitive tasks differed in sensory load, as they contained combined visual and auditory sensory input (videos), as well as only visual input (numbers). Future studies may carefully match affective and cognitive conditions to avoid a difference in sensory load when comparisons between tasks are intended. Regarding affective load, a difference between neutral and sad movies was however intended. Our paradigm does not separate affective valence and affective arousal, as they are collinear. Nevertheless, to approximate subjects' arousal level, we compared MDBF and STAI assessments between affective and cognitive days. Subjects did neither differ in state anxiety (all STAI scores had $P > 0.05$) nor in subjective well-being and wakefulness (all MDBF scores had $P > 0.05$). Hence, findings should be specific to affective valence and not confounded by affective arousal.

Of note, the duration of the baseline scan was 5 min shorter than that of the scans conducted after task, which renders comparisons in dynamic FC for the full length of the measurements impossible. Nevertheless, our approach allowed us to directly compare rest after-task scans using a sufficient number of time points. Future studies should harmonize the durations of all resting-state scans.

As different confound regression strategies may be appropriate in the context of specific scientific goals (Ciric et al. 2016), we based our decision to not perform global signal regression in the absence of further evidence on work by (Braun et al. 2012; Guo et al. 2012), who showed that omission of global signal regression increases test–retest reliability in FC metrics derived via graph theory. Nevertheless, the current results are restricted to the parameters and settings used and the presence of motion artifact and its effects on connectivity should be evaluated within the context of the preprocessing scheme used (Satterthwaite et al. 2013). Future research should aim at identifying denoising strategies, which isolate and remove artifactual global variance while preserving potential "neural" global variance.

Regarding analytical approaches, we chose a network-based analysis, which comes with the advantages of graph-theoretical techniques such as no restriction for choosing regions of interest a priori. Nevertheless, graph analyses are always limited by the underlying parcellation. However, as the current parcellation includes functionally defined nodes placed in 3 major ICNs, it is ideal to evaluate experimental manipulations on the network level and is thus suitable to answer our research question.

Despite the wide use of split- or sliding-window dynamic FC analysis approaches, the absence of gold standards, for example, for setting the ideal window length, is a shortcoming. Short windows lead to more variability, are less able to capture abrupt state transitions, and may give rise to spurious results due to the algorithm itself (Leonardi and Van De Ville 2015; Shakil et al. 2016). On the other hand, long windows may cover rapid effects. As there are no a priori reasons on which one could base the decision how to split the data, this choice is in principle unrestricted. Leonardi and Van de Ville 2015 recommended a sliding-window length of 100 s. However, it was demonstrated that non-stationary fluctuations in FC could also be detected with short windows length such as 40 s, although statistical power is reduced (Zalesky and Breakspear 2015).

Conclusion

To conclude, for the current study clearly shows valence-specific effects of affective stimulation on distinct domains such as subjective feelings, physiological indices in PNS, and functional coupling of brain networks, that jointly constitute an affective experience. Our data demonstrates for the first time that these effects are clearly distinguishable from those of a cognitive task and furthermore provide new insights into carry-over effects of affective stimulation on configuration patterns of functional brain networks, thereby shedding some more light on the trajectory of affective experience, which does not start or end instantaneously.

Supplementary Material

Supplementary data is available at *Cerebral Cortex* online.

Notes

The authors declare no competing financial interests. This work was supported by the German Research Foundation (DFG, Cluster of Excellence "Languages of Emotion"). We thank Dr. Julian Hanich and his team for their help during preparation of the movie clips, and the team at the Center for Cognitive Neuroscience Berlin (CCNB) for their technical support during data acquisition. We thank all participants for taking part in this study.

References

Abramson LY, Metalsky GI, Alloy LB. 1989. Hopelessness depression: a theory-based subtype of depression. Psychol Rev. 96:358–372.

Allen PJ, Josephs O, Turner R. 2000. A method for removing imaging artifact from continuous EEG recorded during functional MRI. Neuroimage. 12:230–239.

Allen PJ, Polizzi G, Krakow K, Fish DR, Lemieux L. 1998. Identification of EEG events in the MR scanner: the problem of pulse artifact and a method for its subtraction. Neuroimage. 8:229–239.

Anand A, Li Y, Wang Y, Wu J, Gao S, Bukhari L, Mathews VP, Kalnin A, Lowe MJ. 2005. Antidepressant effect on connectivity of the mood-regulating circuit: an FMRI study. Neuropsychopharmacology. 30:1334–1344.

Barnes A, Bullmore ET, Suckling J. 2009. Endogenous human brain dynamics recover slowly following cognitive effort. PLoS ONE. 4:e6626.

Borchardt V, Krause AL, Li M, van Tol MJ, Demenescu LR, Buchheim A, Metzger CD, Sweeney-Reed CM, Nolte T, Lord AR, et al. 2015. Dynamic disconnection of the supplementary motor area after processing of dismissive biographic narratives. Brain Behav. 5:1–14.

Braun U, Plichta MM, Esslinger C, Sauer C, Haddad L, Grimm O, Mier D, Mohnke S, Heinz A, Erk S, et al. 2012. Test-retest reliability of resting-state connectivity network characteristics using fMRI and graph theoretical measures. Neuroimage. 59: 1404–1412.

Braun U, Schäfer A, Walter H, Erk S, Romanczuk-Seiferth N, Haddad L, Schweiger JI, Grimm O, Heinz A, Tost H, et al. 2015. Dynamic reconfiguration of frontal brain networks during executive cognition in humans. Proc Natl Acad Sci USA. 112:11678–11683.

Bürger C, Kühner C. 2007. Copingstile im Umgang mir depressiver Stimmung. Zeitschrift für Klinische Psychologie und Psychotherapie. 36:36–45. https://doi.org/10.1026/1616-3443.36.1.36.

Burgess GC, Kandala S, Nolan D, Laumann TO, Power JD, Adeyemo B, Harms MP, Petersen SE, Barch DM. 2016. Evaluation of denoising strategies to address motion-correlated artifacts in resting-state functional magnetic resonance imaging data from the human connectome project. Brain Connect. 6:669–680.

Chang C, Glover GH. 2009. Effects of model-based physiological noise correction on default mode network anti-correlations and correlations. Neuroimage. 47:1448–1459.

Ciric R, Wolf DH, Power JD, Roalf DR, Baum GL, Ruparel K, Shinohara RT, Elliott MA, Eickhoff SB, Davatzikos C, et al. 2016. Benchmarking confound regression strategies for the control of motion artifact in studies of functional connectivity. NeuroImage. 154:174–187. doi: 10.1016/j.neuroimage.2017.03.020.

Disner SG, Beevers CG, Haigh E a P, Beck AT. 2011. Neural mechanisms of the cognitive model of depression. Nat Rev Neurosci. 12:467–477.

Eryilmaz H, Van De Ville D, Schwartz S, Vuilleumier P. 2011. Impact of transient emotions on functional connectivity during subsequent resting state: a wavelet correlation approach. Neuroimage. 54:2481–2491.

Fine JG, Semrud-Clikeman M, Zhu DC. 2009. Gender differences in BOLD activation to face photographs and video vignettes. Behav Brain Res. 201:137–146.

Friedman BH, Thayer JF. 1998. Autonomic balance revisited: panic anxiety and heart rate variability. J Psychosom Res. 44:133–151.

Gärtner M, Rohde-Liebenau L, Grimm S, Bajbouj M. 2014. Working memory-related frontal theta activity is decreased under acute stress. Psychoneuroendocrinology. 43:105–113.

Glover GH, Li TQ, Ress D. 2000. Image-based method for retrospective correction of physiological motion effects in fMRI: RETROICOR. Magn Reson Med. 44:162–167.

Grigg O, Grady CL. 2010. Task-related effects on the temporal and spatial dynamics of resting-state functional connectivity in the default network. PLoS ONE. 5:1–12.

Guo CC, Kurth F, Zhou J, Mayer E a, Eickhoff SB, Kramer JH, Seeley WW. 2012. One-year test-retest reliability of intrinsic connectivity network fMRI in older adults. Neuroimage. 61: 1471–1483.

Gusnard D, Raichle M, Raichle M. 2001. Searching for a baseline: functional imaging and the resting human brain. Nat Rev Neurosci. 10:685–694.

Hamilton JL, Alloy LB. 2016. Atypical reactivity of heart rate variability to stress and depression across development: Systematic review of the literature and directions for future research. Clin Psychol Rev. 50:67–79.

Hamilton JP, Furman DJ, Chang C, Thomason ME, Dennis E, Gotlib IH. 2011. Default-mode and task-positive network activity in major depressive disorder: Implications for adaptive and maladaptive rumination. Biol Psychiatry. 70: 327–333.

Hanich J, Shah M, Jacobsen T, Menninghaus W, Wagner V, Shah M, Jacobsen T, Menninghaus W. 2014. Why we like to watch sad films. The pleasure of being moved in aesthetic experiences. Psychol Aesthetics Creat Arts. 8:130–143.

Harrison BJ, Pujol J, Ortiz H, Fornito A, Pantelis C, Yücel M. 2008. Modulation of brain resting-state networks by sad mood induction. PLoS ONE. 3:e1794.

Hasson U, Nir Y, Levy I, Fuhrmann G, Malach R. 2004. Natural vision. Science. 303:1634–1640.

Hofer A, Siedentopf CM, Ischebeck A, Rettenbacher MA, Verius M, Felber S, Wolfgang Fleischhacker W. 2007. Sex differences in brain activation patterns during processing of positively and negatively valenced emotional words. Psychol Med. 37: 109–119.

Hyett MP, Parker GB, Guo CC, Zalesky A, Nguyen VT, Yuen T, Breakspear M. 2015. Scene unseen: disrupted neuronal adaptation in melancholia during emotional film viewing. NeuroImage Clin. 9:660–667.

Igelström KM, Graziano MSA. 2017. The inferior parietal lobule and temporoparietal junction: a network perspective. Neuropsychologia. 1–14 (in press). https://doi.org/10.1016/j.neuropsychologia.2017.01.001.

Jones DT, Vemuri P, Murphy MC, Gunter JL, Senjem ML, Machulda MM, Przybelski SA, Gregg BE, Kantarci K, Knopman DS, et al. 2012. Non-stationarity in the "resting brain's" modular architecture. PLoS ONE. 7:e39731.

Just N, Alloy LB. 1997. The response styles theory of depression: tests and an extension of the theory. J Abnorm Psychol. 106: 221–229.

Kaiser RH, Whitfield-Gabrieli S, Dillon DG, Goer F, Beltzer M, Minkel J, Smoski M, Dichter G, Pizzagalli DA. 2015. Dynamic resting-state functional connectivity in major depression. Neuropsychopharmacology. 41:1–9.

Kemp AH, Quintana DS, Gray MA, Felmingham KL, Brown K, Gatt JM. 2010. Impact of depression and antidepressant treatment on heart rate variability: a review and meta-analysis. Biol Psychiatry. 67:1067–1074.

Kuehner C, Weber I. 1999. Responses to depression in unipolar depressed patients: an investigation of Nolen-Hoeksema's response styles theory. Psychol Med. 29:1323–1333.

Lavender A, Watkins E. 2004. Rumination and future thinking in depression. Br J Clin Psychol. 43:129–142.

Leech R, Kamourieh S, Beckmann CF, Sharp DJ. 2011. Fractionating the default mode network: distinct contributions of the ventral and dorsal posterior cingulate cortex to cognitive control. J NSci. 31:3217–3224.

Leonardi N, Van De Ville D. 2015. On spurious and real fluctuations of dynamic functional connectivity during rest. Neuroimage. 104:430–436.

Licht CMM, de Geus EJC, Zitman FG, Hoogendijk WJG, van Dyck R, Penninx BWJH. 2008. Association between major depressive disorder and heart rate variability in the Netherlands Study of Depression and Anxiety (NESDA). Arch Gen Psychiatry. 65:1358–1367.

Lindquist KA, Wager TD, Kober H, Bliss-Moreau E, Barrett LF. 2012. The brain basis of emotion: a meta-analytic review. Behav Brain Sci. 35:121–143.

Maron-Katz A, Vaisvaser S, Lin T, Hendler T, Shamir R. 2016. A large-scale perspective on stress-induced alterations in resting-state networks. Sci Rep.. 6:21503.

Montano N, Porta A, Cogliati C, Costantino G, Tobaldini E, Casali KR, Iellamo F. 2009. Heart rate variability explored in the frequency domain: a tool to investigate the link between heart and behavior. Neurosci Biobehav Rev. 33:71–80.

Mullinger KJ, Castellone P, Bowtell R. 2013. Best current practice for obtaining high quality EEG data during simultaneous fMRI. J Vis Exp. (76), e50283. doi:10.3791/50283.

Neumann SA, Waldstein SR. 2001. Similar patterns of cardiovascular response during emotional activation as a function of affective valence and arousal and gender. J Psychosom Res. 50:245–253.

Nolan S, Roberts J, Gotlib I. 1998. Neuroticism and ruminative response style as predictors of change in depressive symptomatology. Cogn Ther Res. 22:445–455.

Nolen-Hoeksema S, Morrow J. 1991. A prospective study of depression and posttraumatic stress symptoms after a natural disaster: The 1989 Loma Prieta earthquake. J Pers Soc Psychol. 61:115–121.

Nolen-Hoeksema S, Davis CG. 1999. “Thanks for sharing that”: ruminators and their social support networks. J Pers Soc Psychol. 77:801–814.

Pehrs C, Deserno L, Bakels JH, Schlochtermeier LH, Kappelhoff H, Jacobs AM, Fritz TH, Koelsch S, Kuchinke L. 2014. How music alters a kiss: Superior temporal gyrus controls fusiform-amygdalar effective connectivity. Soc Cogn Affect Neurosci. 9:1770–1778.

Power JD, Barnes K a., Snyder AZ, Schlaggar BL, Petersen SE. 2012. Spurious but systematic correlations in functional connectivity MRI networks arise from subject motion. Neuroimage. 59:2142–2154.

Power JD, Mitra A, Laumann TO, Snyder AZ, Schlaggar BL, Petersen SE. 2014. Methods to detect, characterize, and remove motion artifact in resting state fMRI. Neuroimage. 84:320–341.

Power JD, Plitt M, Laumann TO, Martin A. 2017. Sources and implications of whole-brain fMRI signals in humans. Neuroimage. 146:609–625.

Raichle ME, MacLeod AM, Snyder AZ, Powers WJ, Gusnard DA, Shulman GL. 2001. A default mode of brain function. Proc Natl Acad Sci USA. 98:676–682.

Sakuragi S, Sugiyama Y, Takeuchi K. 2002. Effects of laughing and weeping on mood and heart rate variability. J Physiol Anthropol Appl Human Sci. 21:159–165.

Satterthwaite TD, Elliott MA, Gerraty RT, Ruparel K, Loughead J, Calkins ME, Eickhoff SB, Hakonarson H, Gur RC, Gur RE, et al. 2013. An improved framework for confound regression and filtering for control of motion artifact in the preprocessing of resting-state functional connectivity data. Neuroimage. 64:240–256.

Schlochtermeier LH, Pehrs C, Bakels JH, Jacobs AM, Kappelhoff H, Kuchinke L. 2017. Context matters: Anterior and posterior cortical midline responses to sad movie scenes. Brain Res. 1661:24–36.

Schulte-Rüther M, Markowitsch H, Shah N, Fink G, Piefke M. 2008. Gender differences in brain networks supporting empathy. Neuroimage. 42:393–403.

Shakil S, Lee CH, Keilholz SD. 2016. Evaluation of sliding window correlation performance for characterizing dynamic functional connectivity and brain states. Neuroimage. 133:111–128.

Shiota MNM, Levenson RW, Leverson R. 2009. Effects of aging on experimentally instructed detached reappraisal, positive reappraisal, and emotional behavior suppression. Psychol Aging. 24:890–900.

Shirer WR, Ryali S, Rykhlevskaia E, Menon V, Greicius MD. 2012. Decoding subject- driven cognitive states with whole-brain connectivity patterns. Cereb Cortex. 22:158–165.

Spreng R, Sepulcre J, Turner G, Stevens W, Schacter D. 2013. Intrinsic architecture underlying the relations among the default, dorsal attention, and frontoparietal control networks of the human brain. J Cogn Neurosci. 25:74–86.

Takano K, Tanno Y. 2009. Self-rumination, self-reflection, and depression: Self-rumination counteracts the adaptive effect of self-reflection. Behav Res Ther. 47:260–264.

Tarvainen MP, Niskanen JP, Lipponen JA, Ranta-aho PO, Karjalainen PA. 2014. Kubios HRV—Heart rate variability analysis software. Comput Methods Programs Biomed. 113:210–220.

Thayer JF, Lane RD. 2000. A model of neurovisceral integration in emotion regulation and dysregulation. J Affect Disord. 61:201–216.

Vaisvaser S, Lin T, Admon R, Podlipsky I, Greenman Y, Stern N, Fruchter E, Wald I, Pine DS, Tarrasch R, et al. 2013. Neural traces of stress: cortisol related sustained enhancement of amygdala-hippocampal functional connectivity. Front Hum Neurosci. 7:1–11.

Veer IM, Oei NYL, Spinhoven P, van Buchem MA, Elzinga BM, Rombouts SARB. 2011. Beyond acute social stress: Increased functional connectivity between amygdala and cortical midline structures. Neuroimage. 57:1534–1541.

Verplanken B, Friborg O, Wang CE, Trafimow D, Woolf K. 2007. Mental habits: Metacognitive reflection on negative self-thinking. J Pers Soc Psychol. 92:526–541.

Wittchen H, Wunderlich U, Gruschwitz S, Zaudig M. 1997. SKID-I. Strukturiertes Klinisches Interview für DSM-IV. Achse I: Psychische Störungen. Göttingen, Germany: Hogrefe.

Xia M, Wang J, He Y. 2013. BrainNet viewer: a network visualization tool for human brain connectomics. PLoS ONE. 8:e68910.

Zalesky A, Breakspear M. 2015. Towards a statistical test for functional connectivity dynamics. Neuroimage. 114:466–470.

Zhang W, Li H, Pan X. 2015. Positive and negative affective processing exhibit dissociable functional hubs during the viewing of affective pictures. Hum Brain Mapp. 36:415–426.